Physical Oceanographic Conditions Drive Patterns of Seasonal Core Habitat Among Marine Top Predators in the San Juan Archipelago

Aidan M. Cox [1]

Pelagic Ecosystem Function Research Apprenticeship
Fall 2021

[1] Friday Harbor Laboratories, University of Washington, Friday Harbor, WA 98250

Contact Information:
Aidan Cox
Aidancox122@gmail.com
(360)-904-8752

Keywords: Species distribution models, suitable habitat map, core habitat, San Juan Archipelago, *Phocoena phocoena*, *Phoca vitulina*, *Larus glaucescens*, *Uria aalge*

Abstract

Species distribution models (SDMs) are valuable tools for characterizing ecological-environmental interactions and identifying regions of core habitat zones of high conservation importance. This is particularly true for marine top predators, organisms at or near the top of their respective food chains, which can be challenging to observe and difficult to manage owing to their relatively low population sizes and highly migratory natures. In this study, I construct species distribution models for the four most abundant species from four predominant families of marine predator across the San Juan Archipelago (SJA). Using a combination of logistic regression analysis and generalized additive models, I describe how nine environmental variables influence patterns of distribution among marine mammals and seabirds respectively and identify regions of core habitat where predators are predicted to be most abundant. Water depth and channel width were identified as highly significant explanatory variables in three of my four SDMs, highlighting the importance of physical habitat structure in the SJA, where strong tidal currents interact with topographical features to create foraging opportunities for piscivorous marine predators. Core habitat zones for multiple predator species occurred almost exclusively within 1-km from shore, suggesting that nearshore areas are critical to ecosystem function from a top-down perspective in this region. Conservation efforts to preserve marine predator populations should focus on restoring altered shorelines to create optimum habitat for marine predators and the forage fish on which they depend. Future shoreline degradation might be prevented by restricting private development of shorelines, with the added benefit of allowing more equitable access to natural spaces where the public can connect with and observe the marine top predators which share their unique ecosystem.

1. Introduction

Understanding patterns and drivers of habitat selection among organisms is critical to understanding ecological systems. Statistical regression models which describe patterns of species distribution (or more simply, species distribution models; SDMs) can be used to identify ecological-environmental relationships and create maps of habitat suitability (Guisan and Thuiller, 2005). As such, SDMs can be used to describe the fundamental ecological niche of species and interpret species interactions and ecological processes where deviations occur (Guisan and Thuiller, 2005; Leathwick and Austin, 2001). SDMs can support effective conservation by identifying core habitat regions, thus improving estimates of population size, trends, and distribution while informing the selection of reserve networks (Ferrier, 2002; Gilles et al., 2016). This is especially true for marine top predators, which generally have small population sizes and occupy large ranges spanning international boundaries, making them both difficult to observe and challenging to manage (Block et al., 2011; Hazen et al., 2018; Shaffer et al., 2006).

The San Juan Archipelago (SJA), located within the temperate inland waters of the Salish Sea bordering the United States and Canada, is a unique coastal habitat which hosts a variety of marine predator species. Four groups of marine predators are predominant year-round within the SJA; these include porpoises (Phocoenidae), seals (Phocidae), gulls (Laridae), and alcids (Alcidae) (Gaydos and Pearson, 2011). These piscivorous predators take advantage of pelagic fish assemblages which thrive in association with seasonally abundant phytoplankton communities (Harvey et al., 2012; Lance and Thompson, 2005; Zamon, 2002). Many narrow channels and shallow sills across the archipelago interact with strong tidal mixing to form jets and eddies which aggregate prey and create foraging opportunities (Mofjeld and Larsen, 1984; Zamon, 2001). Although they share an affinity for the same region, these species display unique life-history patterns. Shifts in the distribution and abundance of top predators such as these can further elucidate subtle environmental changes which propagate through trophic linkages, making them valuable sentinels of ecosystem health (Gilles et al., 2016; Hazen et al., 2019).

The resident marine predators of the SJA possess different life histories suggesting differences in ecological niche and environmental interactions. Porpoises are among the smallest species of toothed whales and inhabit a wide range of marine environments from tropical to temperate latitudes and coastal shelfs to the high seas. Little is known about their reproductive biology and they can be notoriously difficult to observe (COSEWIC, 2016; Elliser and Hall, 2021). Most pinnipeds are known to have strong site fidelity for terrestrial haul out sites and alternate daily between resting on land and foraging at sea (Reidman, 1990). Gulls, the only group of non-diving marine predators considered here, must forage in locations where prey aggregate near the surface or where they can forage in association with other predators. They are commonly provisioned by humans affecting patterns of behavior and distribution (Feng and Liang, 2020). Alcids are a group of diving seabirds and some species can dive up to 100 meters deep (Piatt and Nettleship, 1985). They show strong site fidelity for terrestrial breeding colonies, but migrate widely during most of the year to take advantage of patchy prey resources (Ainley et al., 1996).

A snapshot of habitat use by marine predators is necessary, not only to better understand current patterns of species distribution, but to contextualize future ecosystem change within the SJA. The Salish Sea, including the SJA, is a region currently undergoing extensive ecosystem shifts. The Salish Sea is a highly modified ecosystem subject to numerous anthropogenic pressures including overfishing, shoreline degradation following urban and residential

development, eutrophication, water contamination, and the introduction of non-native species (Gaydos and Pearson, 2011; Harvey et al., 2012; Rice, 2006). Anthropogenic climate change is further driving ocean acidification, increasing surface temperatures, the occurrence and duration of harmful algal blooms – all of which threaten to cause dramatic changes in ecosystem dynamics (Feely et al., 2012; Gobler et al., 2017). Understanding the current distribution patterns of marine top predators will be a useful tool in identifying and assessing these changes to ecosystem function.

In this study I construct and apply species distribution models for four species of marine top predators, in order to explore the environmental drivers of habitat selection and identify regions of core habitat. Here I consider 4 years of abundance data for marine birds and mammals collected along a consistent strip transect running through the San Juan Archipelago. For the most common species in each of four groups (porpoises, pinnipeds, gulls, and alcids) I construct species distribution models, applying logistic regression models to the relatively sparse marine mammals and generalized additive models to the relatively abundant seabird species. Using a combination of 9 static and dynamic environmental variables, I construct seasonal suitable habitat maps for each species in order to identify regions of core habitat for marine predators throughout the SJA. I hypothesize that different environmental variables structure the preferred habitats for each of my study species, reflecting predominant differences in their life histories, but that the highest abundances of predators will overlap in regions of core habitat for marine top predators.

2. Methods:

2.1. Study Area:

My study area covered 1295 km^2 within the Salish Sea, ranging from 122º 43.7' W to 123º 12.3' W and from 48º 43.6' N to 48º 23.6'N. (Fig.1). This area includes all of the major islands of the San Juan Archipelago, an island chain located within the inland waters of Washington state. Located between the Pacific and North American plates, this area experiences dramatic tectonic motion and contains many glacially carved fjords, resulting in a complex network of channels and sills with a highly varied bathymetry profile (ranging from <30-300 meters depth). The Salish Sea is a region rich with fronts, typically defined by persistent patterns of tidal mixing, and coastal upwelling. In Autumn, front patterns shift with prevailing winds, becoming dominated by freshwater input from the Fraser river plume and local downwelling in the late fall and winter (Huyer, 1983). During this period, the highest levels of primary production are generally observed in the north of my study area where riverine inputs supply the necessary stratification and nutrients to support a fall phytoplankton bloom, which generally occurs in mid-late October (Boldt et al., 2019). Persistently high primary productivity is found in the shallow sounds of Orcas Island. Using QGIS, I subdivided this study area into 1 km^2 grid cells and isolated marine habitat by excluding cells with an average elevation or centroid located above sea level.

2.2. Field Methodology:

Within this study area, a consistent strip transect was conducted approximately six times annually from 2008 to 2021 during October and November to monitor the abundance of predators from two taxonomic guilds, marine mammals and seabirds. This strip transect covered an area of 8.4 km^2 which was subdivided into six zones corresponding with prominent topographic and bathymetric habitat features (Table 1). Transects were performed onboard a 42-

foot modified research vessel, the 'Kittiwake' based out of Friday Harbor Laboratories. The transect line was driven twice each cruise day, once from N-S and again from S-N. On each transect, a minimum of two undergraduate students were stationed on the port and starboard sides of the ship's upper deck. These students acted as primary observers and were often accompanied by data recorders and supporting observers. Observers monitored the area within 200 meters ahead of and perpendicular to the ship. Species identification, number of individuals and time were recorded for marine birds and mammals sighted within this search area. Species spotted on land were not considered. Species counts were transformed into density (indiv. km^{-2}) values for each transect zone to account for differences in survey effort between zones. 28 species of marine mammals and seabirds were monitored during these surveys, however in this analysis, I focus specifically on the four most common predator species from four families. These included harbor porpoise (*Phocoena phocoena*; Phocoenidae), harbor seal (*Phoca vitulina*; Phocidae), glaucous-winged gull (*Larus glaucescens*; Laridae), and common murre (*Uria aalge*; Alcidae). New observers were conscripted annually from the students studying marine birds and mammals as part of the Pelagic Ecosystem Research Apprenticeship at Friday Harbor Labs and were trained the week prior to the first transect was conducted. Only abundance data from 2017-2021 were considered here to match the availability of my most restrictive environmental variables.

2.3. Environmental Data:

A combination of 9 static and dynamic environmental variables were considered as explanatory variables when modeling the abundance of marine bird and mammal species (Table 2). Variables were identified based on previous student projects and published literature. Values for each environmental variable were averaged within the grid cells of our study area at 24-hour resolution for all days between October and November to match the time when transects were conducted.

Static Variables: Water depth, bottom topography, channel width, distance from shore and water depth variability (measured as the standard deviation of bathymetry) were included as proxies for physical habitat structure, as well as for their influence on the flow of water through the study area. Bathymetry data for U.S. waters were extracted from the National Oceanic and Atmospheric Administration (NOAA, https://www.ngdc.noaa.gov/mgg/coastal/crm.html) Coastal Relief Model while values from Canadian waters were taken from the British Columbia Digital Elevation database (https://www2.gov.bc.ca/gov/content/data/geographic-data-services/topographic-data/elevation/digital-elevation-model). These data were processed using QGIS software (QGIS Development Team, 2021) and values for each grid cell were extracted or manually calculated. Another static variable, tidal current amplitude, was included as a proxy describing the strength of tidally driven movement across my study area. To calculate this variable, I extracted tidal current speeds from 40 tidal prediction stations operated by NOAA (https://tidesandcurrents.noaa.gov/noaacurrents/Stations?g=698). These data were available from 2019-2021. Daily current amplitude was calculated from the maximum flood and ebb speeds and values from October to November were averaged at each tidal station to create a seasonal proxy for tidal current strength. A one-way ANOVA was used to compare these annual seasonal averages across 2019-2021 to determine if strong interannual differences in tidal strength existed at each location and no significant difference was identified ($p = 0.975$). Finally, the seasonal tidal amplitude at each station was averaged across 2019-2021 to create a final static proxy for

tidal current amplitude at each station. Tidal amplitude values from the nearest tidal station were applied to each grid cell in our study area.

Dynamic Variables: Sea surface temperature and surface salinity were included for their role in identifying the unique water masses which converge across the San Juan Archipelago. In this region, warm, fresh water from the Fraser river plume and cool, salty water from the Strait of Juan de Fuca are commonly mixed by wind stress and tidal forces, driving patterns of water stratification and primary productivity . From these data, the standard deviation of sea surface temperature within each grid cell was calculated as a proxy for frontal zones where water from different origins, with different temperature profiles meet. Lastly, chlorophyll concentrations at the surface were included as a proxy for water column productivity. Across these four variables, surface values were exclusively considered since they are sufficient to identify water from different origins (Schulien et al., 2020). Furthermore, incident light is greatest at the surface; thus, this is where most primary production occurs, and where trophic interactions are limited for the non-diving predators included in my models. Considering only surface values also reduced the amount of data handling and processing required for analysis. Values for my four dynamic variables were obtained from LiveOcean, a high-resolution regional ocean model for the Salish Sea. The LiveOcean model produces data at a spatial resolution of 0.25 km^2, resulting in four data points within each of my study grid cells. Daily values for each variable were averaged across these four points, resulting in a single value for each grid cell. Archival data from LiveOcean were only available from January 2017 through October 2021, thus, data were extracted from October to November from 2017-2020 and October of 2021.

2.4. Data Analysis:

All data analysis was performed using R, version 3.5.3 (R Core Team, 2019). Different model types were chosen to describe the abundance of marine mammals and seabirds in relation to my explanatory environmental variables. Particularly for marine mammals, there were substantial amounts of zero values (absences) across the dataset. Between 2017 and 2021, thousands of seabirds were spotted cumulatively, while marine mammals were sighted only a few hundred times. For the less frequently observed marine mammals, binomial logistic regression models were selected, where species presence was the response variable. For the relatively abundant seabird species, generalized additive models (GAMs) were constructed using species density as the response variable.

I averaged the values of my explanatory variables across the grid cells within each transect zone for each date transects were conducted. This ensured that the spatial resolution of my explanatory variables matched the resolution of my response variables. Thus, data on marine predator abundance and marine environmental conditions were available for 28 cruise dates, conducted between 2017 and 2021. Before beginning model construction, I conducted a pairwise linear correlation analysis across my nine explanatory variables in order to identify collinearity ($r \geq |0.5|$). Large outliers in marine bird and mammal density estimates were identified as any values greater than the 75^{th} percentile by more than 1.5 times the interquartile range. These values were replaced with the nearest, non-outlying value.

I randomly selected 75% of these data (21 days) to be used in model training, resulting in a training sample size of 126 data points (6 zones day^{-1}). Both types of models were constructed using forward selection of explanatory variables whereby variables were added individually to the model with only the best predictor being retained at each iterative stage of model development. Model comparisons were performed based on AIC weights (Wagenmakers and

Farrell, 2004). After each iteration, the best predictor was added to the model and any collinear variables were eliminated from further consideration. The final model was identified as the iteration with the lowest AIC where all predictors were statistically significant ($\alpha < 0.05$). In cases where the ΔAIC weight < 20, the most parsimonious model was selected (Pearce and Ferrier, 2000).

Logistic Regression Models: Logistic regression analysis was used to describe patterns of distribution among marine mammals, using probability of habitat occupancy as the response variable. Presence vs. absence of harbor seals and harbor porpoises within each transect zone on each cruise day were used as the dependent variable in model training. A binomial distribution family was used in conjunction with generalized linear modeling to develop these SDMs and was chosen to reflect the two outcomes which can be realistically predicted (species presence and species absence). A linear relationship between the response variable and each explanatory variable was considered initially following the recommendation of other researchers (Hosmer et al., 1989) to prevent overfitting against data containing a high proportion of species absences. Generalized linear models were maintained after the results of generalized additive modeling (which can accommodate non-linear relationships) revealed many near linear correlations between response and predictor variables for seabird abundance.

Generalized Additive Models (GAMs): Generalized additive models (Hastie and Tibshirani, 1990), (mgcv library in R; Wood, 2003) were used to describe seabird abundance across my study area, using the density of common murres and glaucous winged gulls as response variables. An extension of generalized linear models, GAMs are often used to construct species distribution models for their ability to describe complex, non-linear relationships between response and prediction variables (Guisan et al., 2002). The Poisson distribution family was selected to construct my GAMs for its utility in modeling species counts. The Poisson distribution can only produce predictions which are positive, real numbers because it is based on a minimum value of 0 and contains only integers. Similarly, species counts can only be 0 (absent) or positive, real numbers. Although my GAM models are built using species density as a response variable rather than species counts, when applied to my study grid of 1 km^2 grid cells, these densities (indiv. km^{-2}) are essentially converted into direct counts. Default, thin-plate regression splines were used as smoothing terms for each of my environmental variables. The minimum number of knots (3) were applied to static variables which had only 6 levels of x (one average for each zone with no temporal variability) to prevent overfitting. Similarly, 4 knots were applied to dynamic variables which still allowed my models to describe a variety of non-linear relationships.

Seasonal Habitat Maps: I applied my final models to daily values for each predictor across each grid cell in our study area in order to make daily predictions of habitat-use across my study area. I then averaged these daily predictions for each grid cell across all days in October and November from 2017-2021 to create a seasonal, predicted habitat map for each species. Predictions for each species in each guild, marine mammals and seabirds, were averaged to create similar habitat maps for each predator guild. Grid cells within the 90th percentile of predicted values for these guild habitat maps were selected and used to identify core habitat regions for marine mammals and seabirds across the San Juan Archipelago

2.5. Model Validation:

Species Distribution Models: To assess the accuracy of my species distribution models, I utilized a simple, holdout validation approach for its computational ease and conceptual accessibility. I

applied my models for each individual predator species to environmental data from the remaining 25% of cruise days not utilized in model training to make predictions of occupancy within each zone (in units of density for seabirds and probability of presence for marine mammals). For seabird distribution models I performed a paired t-test comparing predicted density values with observed density values in each zone on each cruise date (n = 42). For marine mammal distribution models, I performed a similar paired t-test, however here I compared the proportion of cruises in which each species was sighted within each transect zone and compared these to model predictions for probability of presence within each zone (n = 6). Because my comparisons for marine mammal distribution models were based on very small sample sizes, I confirmed the normality assumption of the paired t-test was met by applying a Shapiro-Wilk test to the differences between observed and predicted values.

LiveOcean: To assess the accuracy of modeled environmental data on which my models were built, I performed a similar validation using data obtained from LiveOcean. I compiled measured physical oceanographic data from 67 CTD casts conducted between 2017-2021 concurrently with marine predator plot transects. CTD deployments were conducted at the northernmost and southernmost ends of the transect line and were therefore referred to as north and south stations respectively (Table 1). Across each CTD deployment, I extracted the shallowest temperature and salinity values recorded (ranging from 0.5 - 5 meters depth). For comparison, I extracted LiveOcean data from the 4 locations closest to each station and averaged values for each day CTD data were collected. Using a paired t-test, I tested the difference between observed and modeled values at each station on each day.

Cluster Analysis: K-means clustering was used to compare the environmental conditions and identify regions with similar environmental characteristics across my study area. This was used primarily to determine if the conditions encountered along our transect lines were representative of the conditions across the rest of my study area. I normalized each of my explanatory variables to a mean of 0 and standard deviation of 1 before clustering. Using the R package factoextra (Kassambara and Mundt, 2020), I calculated the within cluster sum of squares for k values between 1 and 10 and chose the lowest k-value for which there was a substantial decline in within cluster variation. Principal components analysis was also used to visually compare the separation between clusters in order to confirm that my selected k-value minimized cluster overlap.

3. Results:

3.1. Correlation among environmental variables

Pairwise Pearson's linear correlation analysis revealed a high degree of correlation between my explanatory environmental variables. Of the 36 possible pairwise variable combinations 35 revealed statistically significant correlations with three variable combinations being moderately to strongly correlated ($|r| \geq 0.5$) (Table 3). For brevity, I will describe only these moderate to strong correlations here. (1) Channel width increased as distance from shore increased. (2) Chlorophyll concentration increased in close association with sea-surface temperatures but (3) decreased in waters with higher levels of surface salinity.

3.2. Transect Characteristics and Results

Between October of 2017 and October of 2021, line transects were conducted on 28 cruises, resulting in 28 observations within each of our 6 zones for a total dataset of 168 observations. The distribution of survey effort was not identical across years owing to differences in weather

conditions, availability of vessels, and the occurrence of the COVID-19 pandemic. Table 4 contains a list of survey conditions and effort across each year included in my analysis. Across these transects, marine mammals were observed to be present 409 times (476 harbor seals and 164 harbor porpoises were sighted). Seabird species were spotted 3241 times and a total of 15,101 individuals were observed (5137 glaucous-winged gulls and 9965 common murres). Temperature and salinity data collected from CTD casts at two stations on each cruise day were significantly different from data at the same location obtained from the LiveOcean model (paired t-test, $p < 0.001$). The mean difference between model predictions and observations was -0.26 ºC and 0.54 PSU for temperature and salinity respectively.

3.3. Marine Predator Occurrence Patterns

Harbor Porpoise: Across my dataset, harbor porpoises were most commonly observed outside of Friday Harbor, in zone 2 of our transect line, and least commonly observed in the Strait of Juan de Fuca at zone 6 of our transect line (42% and 10% of days respectively). The highest density of harbor porpoises was also observed in zone 2 of our transect (0.284 indiv. km^{-2}). The distribution of harbor porpoises was highly variable between years in our study. Across individual years, the highest number of harbor porpoise sightings occurred in zone 4 (2017), zones 2,3, and 5 (2019, 2021) and zone 2 (2018, 2020). Distance from shore was the only statistically significant explanatory variable identified for inclusion in the logistic regression model for harbor porpoises ($p = 0.02$) (Table 5), with an odds ratio of 0.998 (95% confidence interval: 0.997 – 0.998) (Fig.2). This model explained 4.6% of the variation in harbor porpoise distribution. 25% of harbor porpoise observations occurred in zone 2, within 600 meters from shore. Based on this model, the predicted probability of encountering a harbor porpoise in zone 2 was 0.41 compared to 0.08 in zone 6, which was ~2000 meters from shore. Holdout validation revealed no significant difference between the proportion of sightings in each zone and the model's predicted probability of presence (paired t-test, $p = 0.20$). A Shapiro-Wilk test confirmed that differences between observed proportion of occupancy and predicted probability of occupancy within each zone were normally distributed ($p = 0.07$).

Harbor Seal: Harbor seals were most commonly observed in Griffin Bay, zone four of our transect (82% of days), a pattern which was consistent across all study years except one (2019, zone 5). Harbor seals were seen least frequently in the Strait of Juan de Fuca, zone 6 of our transect (10% of transects). Three environmental variables were identified as significant predictors in the logistic regression model for harbor seal distribution (Table 5). These were depth ($p < 0.01$), channel width ($p < 0.001$), and tidal current amplitude ($p = 0.01$). Harbor seal presence was negatively correlated with water depth (odds ratio: 0.956, CI: (0.926 - 0.988) and channel width (odds ratio: 0.999, CI: 0.999 - 0.999) but positively correlated with tidal current amplitude (1.92, CI: 1.11 – 3.30) (Fig.2). This model explained 23.7% of the variability in harbor seal distribution. Holdout validation revealed no significant difference between the proportion of sightings in each zone and the model's predicted probability of presence (paired t-test, $p = 0.82$). A Shapiro-Wilk test confirmed that differences between observed proportion of occupancy and predicted probability of occupancy within each zone were normally distributed ($p = 0.71$).

Common Murre: Common murres were the most abundant seabird observed along our transect line in every year considered. Murres were most abundant in the Strait of Juan de Fuca, zone six of our transect line, where 20.2 indv. km^{-2} were sighted on average (sd = 13.6 indv. km^{-2}). Common murres were frequently sighted in small aggregations with an average group size of 5 individuals. Four environmental variables were included in the best predictive model for

common murres including smoothed components of water depth, chlorophyll concentration, channel width, and SST standard deviation (Table 5). The predicted density of common murres was highest over water 80 meters deep, in channels > 1-km wide. Common murre abundance increased with chlorophyll concentration and decreased as SST standard deviation increased (Fig.2). The generalized additive model for common murre density described 30.9 % of the variability in observed abundance. Holdout validation revealed no significant difference between observed density and model predictions (paired t-test, $p = 0.64$).

Glaucous-winged gull: Glaucous gulls were observed in the highest abundance in zone five of our transect line, which passes through Cattle Pass, San Juan Island. From 2017-2021 16 indv. km^{-2} were observed in this area on average (sd = 9.1 indv. km^{-2}). Variability in the abundance of glaucous-winged gulls was substantially higher within years than between years as determined by a comparison of the within and between year sum of squares (10100 and 702 respectively). Six of my nine environmental variables were identified as highly significant predictors of glaucous-winged gull density. My best predictive model included smoothed components of water depth, channel width, sea-surface temperature, salinity, SST standard deviation, and topography (Table 5). The predicted density of glaucous gulls peaked at surface temperatures of ~10 ºC with low temperature variability, and salinities exceeding 31.5 PSU. Gull abundance decreased with increasing water depth and increased with increasing channel width. Higher densities also occurred in cells with relatively high bottom topography (~25 m) (Fig.2). This model explained 30.5% of the variability in glaucous-winged gull abundance. Holdout validation revealed a significant difference between observed density and model predictions (paired t-test, $p < 0.01$).

3.4. Seasonal Habitat Predictions

Harbor porpoise: The average predicted probability of encountering a harbor porpoise on any given day between October and November across my study area grid was 0.238 (sd = 0.200) and ranged from 0 to 0.602. The highest predictions of habitat occupancy for harbor porpoises occurred around the periphery of each major island, with predicted probability decreasing moving away from shore (Fig.6). Predictions equal to or greater than 0.529 fell within the 90th percentile, indicating that across 10% of my study area, harbor porpoises are predicted to be present on 50% of days between October and November. These areas fell within 1 km of shore of each of the major San Juan Islands, including San Juan, Orcas, Lopez, and Shaw.

Harbor seal: Predicted probabilities of harbor seal presence ranged from 0 to 0.998 across my study area and had an average of 0.430 (sd = 0.402). This suggests that across our study area, there is a 43% chance of encountering a harbor seal on any given day between October and November. The highest predictions for harbor seal habitat occupancy occurred within the interisland channels, particularly those on the eastern side of my study area separating Shaw, Orcas, and Lopez islands (Fig.6). Grid cells within the 90th percentile had predictions greater than or equal to 0.970 and occurred within the shallow sounds of Orcas and Lopez islands, as well as at channel constriction points such as Cattle Pass, Wasp Passage, and Obstruction Pass.

Common Murre: Predicted densities for the common murre ranged from 0 to 50.4 birds km^{-2} across my study area. The average predicted density of murres between October and November across all grid cells was 10.4 birds km^{-2} (sd = 10.5). The highest predicted densities for common murres were distributed throughout Rosario Strait, particularly in the southern end of my study area near Deception Pass (Fig.6). The 90th percentile of density predictions included

values greater than or equal to 28.0 birds km^{-2}. These areas were concentrated along the eastern periphery of my study area, 1-6 km from shore from Lopez and Orcas islands. A small cluster of grid cells ~ 8 km southwest of San Juan Island, in the Strait of Juan de Fuca were also predicted to support common murre densities within the 90th percentile.

Glaucous-winged gull: The average predicted density of Glaucous-winged gulls throughout my study area between October and November was 7.64 birds km^{-2} (sd = 9.34 birds km^{-2}) and density predictions ranged from 0 to 78.1. The predicted density of glaucous-winged gulls was relatively homogenous across the majority of my study area, with spikes in predicted abundance surrounding the mouths of interisland channels (Fig. 6). Here, density predictions greater than or equal to 17.7 birds km^{-2} fell within the 90th percentile. Grid cells within this category were concentrated within the Strait of Juan de Fuca off of San Juan and Lopez islands between 1 and 7 km from shore.

Combined: Several grid cells fell within the 90th percentile for more than one study species and were thus considered to be core habitat for marine top predators. Thirty-two grid cells were predicted to be core habitat for both species of marine mammals considered here. These areas were distributed around the shallow bays and sounds of Lopez and Orcas Island as well as channel constrictions with strong tidal current amplitudes, including Lopez, Obstruction, and Wasp passages. The core habitats of marine mammals and seabirds overlapped in a total of 23 grid cells. These overlaps occurred at bays, beaches, and headlands with a wide variety of conditions distributed throughout my study area. Core habitat for both species of seabirds considered here occurred in 10 cells located within Haro and Rosario straits, typically several kilometers from shore. Finally, five cells were predicted to be core habitat for three species of top predator, harbor porpoises, harbor seals, and glaucous gulls. These regions of triple overlap were predicted to occur in the Figure 7 displays; these regions of habitat overlap between each combination of predator species.

3.5 Cluster Analysis

K-means cluster analysis revealed a total of 5 habitat clusters of similar environmental regimes across my study area (Fig 8). Cluster 1 was located in the southern region of my study area, nearest to the Strait of Juan de Fuca and included the widest channel of our study area, the largest overall distance from shore, and highly saline waters (Table 6). Cluster 2 occurred northward, in Haro Strait on the west side of San Juan Island and included the deepest subsurface glacial fjord in my study area. As such, it boasted the greatest average depth and bottom topography, as well as the lowest level of surface chlorophyll concentration. Most of my study fell within a third cluster, which extended from Friday Harbor westward across my study area. The conditions in cluster 3 were the closest to the average across my study area, however this cluster included many narrow passages and as such, had the highest average tidal current amplitude of any cluster. The shallow sounds of Orcas Island were identified as their own unique habitat type, cluster 4. These regions were characterized by the highest average primary productivity in my study area as well as the narrowest channels and shallowest waters. Lastly, cluster 5 occurred in the northernmost extent of my study region, extending from the tops of San Juan and Orcas Islands north into the Strait of Georgia. This cluster was defined by the highest variability in sea-surface temperature of any cluster, as well as the slowest tidal current amplitudes and lowest salinity values. Marine predator strip transects conducted in this study fall within the area of clusters 2, 3, and 5. Cluster 4 had the highest predicted abundance of all

predator species considered here, except for common murres which were predicted to be most abundant in cluster 3.

.

4. Discussion

4.1. SDMs

All nine environmental variables included in this analysis were identified as significant predictors of marine predator abundance in one or more species distribution models. Water depth and channel width were the two variables most commonly included in my final predictive models, identified as highly significant predictors of habitat use for three of my four study species. This suggests that the interaction between water movement and topographical features may be the most important determinant of habitat structure for marine predators across the San Juan Archipelago. The standard deviation of sea-surface temperature was the next most commonly included variable, appearing in both SDMs for my two seabird species. Regions of high temperature standard deviation reflect regions where water masses with different temperature profiles mix together. These regions of persistent mixing supported lower concentrations of chlorophyll suggesting lower throughput of energy to higher trophic levels (Harvey et al., 2012). Seabirds, which occupy a lower trophic level than the marine mammals considered here, may be more closely coupled to phytoplankton abundance and therefore more influenced by these regions (Feddern et al., 2021; Gulka et al., 2019; Nichol et al., 2013; Zamon, 2003). Each model included a slightly different combination of environmental predictors, reflecting the unique life history and foraging strategies of the four species of marine predators considered here.

Harbor porpoise: The suitable habitat predictions for harbor porpoises described here are reflective of their ecological niche piscivorous apex predator in shallow coastal waters. The highest predicted probabilities of habitat occupancy for harbor porpoise occurred within 1 km from the major islands and rocks of the San Juan Archipelago, decreasing in probability at greater distances from shore (Fig.2). Similar studies have found that harbor porpoises remain closely associated with coastal waters throughout the year and remain within the 200-meter depth isobath even during summer months, when their distribution is extended (Spyrakos et al., 2011; Tynan et al., 2005). In the North Atlantic, harbor porpoise distribution patterns have also been successfully modeled, including distance from shore as a predictor (Marubini et al., 2009). In at least one instance, researchers found that distance to sand lance habitat may be a better predictor than distance from shore, suggesting that porpoises use nearshore environments as foraging grounds (Gilles et al., 2016). Although the diet of Harbor porpoises is not fully categorized in the Salish Sea, this species is known to forage on Pacific herring (*Clupea pallasii*), hake (*Merluccius productus*), pollock (*Gadus chalcogrammus*), and salmon (*Oncorhynchus spp*.) (Elliser et al., 2020; Nichol et al., 2013). These and other species of pelagic forage fish are commonly found close to shore in the San Juan Islands (Fletcher, 2021; Stasko et al., 1976). Despite this ecological precedent, the identification of distance from shore as a significant predictor of harbor porpoise distribution may also be a product of observer bias.

A violation in the basic assumptions of plot sampling could also explain the correlation between porpoise habitat occupancy and distance from shore, by resulting in a biased estimate of species density in some zones. Harbor porpoises are a notoriously cryptic species which can be difficult to spot and are known to be harder to spot in regions with higher sea states (rougher water (COSEWIC, 2016; Elliser and Hall, 2021). Our observers may have missed harbor porpoises when they were present along our transect line, particularly in zone six, a tidally active

region relatively far from shore of the Strait of Juan de Fuca. Here, sea-states were observed to be higher on average than other zones along our transect line making it more difficult to spot porpoises surfacing. This would violate a key assumption of plot sampling, that all organisms along the transect line are spotted, resulting in lower estimates of abundance. Pearson's linear correlation analysis revealed that there was no significant correlation between the predicted probability of habitat occupancy for harbor porpoises and the density which was observed in each spatial zone of our transect ($p > 0.05$, $r = 0.12$), suggesting that porpoises may not have been more abundant in regions where they were sighted more frequently but rather may have been more easily spotted in regions where they were present.

Surprisingly, no significant relationship between tidal current strength and porpoise abundance was identified here despite findings in other regions. Previous studies in tidally dynamic regions of the North Atlantic have found that harbor porpoise distributions are likely to be associated with areas of high tidal activity (Johnston et al., 2005; Marubini et al., 2009; Scott et al., 2010). Studies of other piscivorous predators in the San Juan Archipelago found significant influence of tidal state on animal behavior and foraging activity (Zamon, 2003, 2001). Here, tidal current amplitude had a negative correlation with the probability of harbor porpoise presence, whereby porpoises were less common in regions of strong tidal currents. This relationship was not statistically significant and was thus eliminated after the first round of model selection ($p = 0.18$). Other research using the same dataset but including additional years of abundance data (2008-2021), found that tidal current direction was a more important predictor of porpoise presence than was tidal current strength. The same research also suggested that there may be a recent shift and decreased influence of tidal current on porpoise distribution (Frederick, 2021).

Harbor Seals: The best model predicting harbor seal distribution included three variables which closely reflect their life history as small, coastal pinnipeds. Water depth, channel width, and tidal current amplitude were identified as highly significant predictors of harbor seal distribution, with seals being more common in shallow water of narrow channels with fast tidal currents (Fig.3). Like other pinnipeds, harbor seals alternate daily between terrestrial haul-out sites and marine foraging grounds (Riedman, 1990), and thus, their energetic gain is limited by the distance between these two habitat types. This explains the close association with harbor seals and nearshore environments. Harbor seal foraging is also known to be associated with tidal state, and research conducted at Cattle Pass, San Juan Island - a site within zone 5 of our transect line - suggests that the interaction between current speed and channel width may create additional foraging opportunities for harbor seals (Zamon, 2001). Interestingly, harbor seal foraging success was observed to be greatest during periods of slower daily flood tides. Harbor seals were not observed to be more common in the water during slower tides, and thus, this observation does not necessarily contradict my finding (given that harbor seals could select for the slowest daily tide within regions of overall strong tides); however, it does suggest that there may be additional variability in the relationship between harbor seals habitat use and tidal current strength which is not captured by my model.

The seasonal habitat map for harbor seals (Fig.6) constructed here predicts a high probability of habitat occupancy across much of my study area, suggesting that the San Juan Archipelago (SJA) likely offers abundant habitat for harbor seals. Across my study area, 25% of predictions for habitat occupancy among harbor seals were above 0.88. This suggests that Harbor seals have an 88% chance of being encountered on any given day between October and November across a cumulative area of approximately 200 km^2 within the SJA. The San Juan Archipelago may

support a population of as many as 7000 harbor seals and thus, the high predicted probability of harbor seal occupancy across my study area may fall within realistic expectations (Lance and Jeffries, 2007) . Based on these predictions, the physical habitat of the SJA likely provides abundant habitat for harbor seals

Common Murre: The seasonal habitat map for the common murre (Fig.6) reflects their ecological niche as a diving seabird, and predator of small, pelagic forage fish. Murres distribution was best explained by four variables, water depth, channel width, chlorophyll concentration, and sea-surface temperature standard deviation (Fig.4). Unlike other predators considered here, murre abundance was strongly positively correlated with chlorophyll concentration. This could be because murres occupy a lower trophic level than other diving predators considered in this study, foraging primarily on Pacific herring, Pacific sand lance (*Ammodytes personatus*), and juvenile salmonids (Gulka et al., 2019; Lance and Thompson, 2005). Phytoplankton are known to have high energy throughput in the SJA, and areas with high levels of primary production may attract large aggregations of planktivorous forage fishes (Harvey et al., 2012). Across my study area, common murres were predicted to be most abundant in channels at least than 1-km wide, over water ~80 meters deep. Several areas which meet these conditions appear to occur near subtidal wavefields which serve as key habitat for pacific sand lance (Baker et al., 2021; Greene et al., 2020).

Many other species of resident, pursuit-diving birds inhabit the SJA, and it is unclear from these models if spatial partitioning of resources occurs across my study area. Species which occupy the same ecological niche cannot coexist without competition and thus, species may develop behavioral adaptations to reduce overlap in one or more dimensions (Gause, 1971, 1934). Rhinoceros auklets (*Cerorhinca monocerata*) marbled (*Brachyramphus marmoratus*) and ancient murrelets (*Synthliboramphus antiquus*), as well as pelagic (*Phalacrocorax pelagicus*) and double-crested cormorants (*Phalacrocorax auratus*) all inhabit the San Juan Archipelago and occupy a similar ecological niche (Gaydos and Pearson, 2011; Lance and Thompson, 2005). Research shows that murres may spatially segregate foraging by time of day, dive, depth, and location (Gulka et al., 2019; Lance and Thompson, 2005). Without including species interactions as explanatory variables, species distribution models such as those constructed here can only model the fundamental habitat of a species. The realized habitat, to which a species is confined by competitive exclusion, may be much different. My models highlight the suitable habitat for common murres and other pursuit diving seabirds, however more data is needed to determine how different species segregate in space and time across these core habitat zones.

Glaucous-winged gull: As the only non-diving predator considered in this study, the suitable habitat of glaucous-winged gulls (Fig.6) reflects regions of increased foraging opportunity for a surface-seizing predator. Seabirds are known to exhibit site fidelity to tidal features such as rips and jets, and glaucous-winged gulls specifically have been observed to forage in association with tidal jets in the SJA (Irons, 1998; Zamon, 2003). Tidal jets form where tidal currents interact with topographic features such as headlands, promontories, and steep-sided channels. In this study, my models predict glaucous-winged gulls to be most abundant in shallow waters of wide channels (Fig. 5). Across my study area, water depth generally increased with distance from shore ($r = 0.22$, $p < 0.001$), suggesting that glaucous gulls are likely to be found close to shore where narrow interisland channels open into the wider, outlying straits. Glaucous-gulls were also predicted to be more abundant in areas with variable bottom topography, such as regions with steep-sided channels, further reflecting their association with tidal jets. During flood tides, these regions may serve as foraging grounds for pelagic forage fish, which become simultaneously

more distributed in the water column and visible to predators from the surface while feeding (Zamon, 2003).

The large variability in observed abundance of glaucous-winged gulls suggests that more environmental and ecological interactions structure the distribution of this species than are currently included in my models. Although common murres were the most frequently observed seabirds on our transect, gulls were present in large numbers occasionally. While conducting transects, we observed large aggregations of gulls foraging in association with diving marine predators such as Steller sea lions (*Eumetopias jubatus*), harbor porpoises, and humpback whales (*Megaptera novaeangliae*). Gulls were also observed in association with humans, as large flocks were commonly observed following crabbing and fishing boats. These observations suggest that gull aggregations may be, at least in part, dependent on transient or incidental foraging opportunities in association with other species. Glaucous winged gulls had the most variable patterns of abundance of any species considered in this study and were the only species for which model predictions were significantly different from observed densities ($p = 0.002$). The inclusion of more environmental variables and species interaction terms may be necessary to accurately model the distribution of this particular species.

4.2. Seasonal Core Habitat Maps

Despite differences in the environmental predictors that were most significant for each of my study species, the regions of highest predicted abundance overlapped for several of my study species. Harbor seals and harbor porpoises had the greatest overlap of any two species (32 grid cells within the 90th percentile of probability of habitat occupancy by both species) , likely reflecting their relatively similar life histories, prey types, and foraging strategies. Regions with high predicted occupancy by marine mammals also overlapped extensively with areas of high predicted seabird densities (23 grid cells). These regions of overlap were distributed widely around the SJA but occurred exclusively within 1 kilometer from shore. This suggests that the four species of marine predators considered here may be particularly susceptible to direct interaction and conflict with humans, such as noise pollution, vessel strikes, entanglement, and exposure to pollution (Alava, 2019; Olson et al., 2021; Selden, 2021). Predators may also be susceptible to more indirect conflicts as a result of their dependence on nearshore habitat, such as shoreline habitat degradation. For example, research shows that altered beaches serve as poor spawning habitat for pacific surf smelt which utilize similar spawning grounds as Pacific sand lance, a critical prey resource for marine mammals and seabirds in this region (Rice, 2006).

Compared to marine mammals, habitat overlap between glaucous-winged gulls and common murres was less extensive (10 grid cells) and occurred farther from shore. A majority of the grid cells within the 90th percentile of predicted density for both glaucous-winged gulls and common murres (6/10) occurred >3 km from shore in the Strait of Juan de Fuca at the southern end of my study area. These offshore core habitat regions for seabirds occurred near or within active shipping lanes. With a potential increase in shipping traffic as a result of the approved expansion of the Kinder Morgan Trans-mountain pipeline, seabirds in this region could face increased disturbances from vessel traffic (Bertram, 2020). The predicted core habitat for seabirds in this study spanned the international boundary between the United States and Canada, which could complicate efforts to conserve the habitat of these species, illustrating a common issue in the conservation of marine predators.

Species distribution models constructed here reflect the suitable habitat of predators between the months of October and November, and patterns of habitat use may differ on

seasonal and annual scales. The movements of other, seasonally abundant conspecific species may affect competition for resources and thus influence patterns of distribution. For example, Pacific-white sided dolphins (*Lagenorhynchus obliquidens*) occupy a similar ecological niche to harbor porpoises and occur in greater densities throughout the Salish Sea in fall and winter. In the summer, when the distribution of dolphins expands to take advantage of offshore productivity, harbor porpoises may occupy a wider habitat range in the SJA (Ashe, 2020; Gaydos and Pearson, 2011; Tynan et al., 2005). Similarly, Steller sea lions and Northern Fur seals (*Callorhinus ursinus*) are more common in the Salish Sea in fall and winter months, potentially restricting the habitat availability for harbor seals during these seasons (Gaydos and Pearson, 2011). Patterns of species abundance and distribution may also vary in response to annual reproductive cycles. Harbor seals are known to become more gregarious during the breeding season (generally in mid-summer) and may therefore become more condensed in their distribution (Riedman, 1990; Teilmann and Galatius, 2018). Similarly, common murres exhibit high site fidelity for specific terrestrial breeding colonies, which attract colonies of tens-of-thousands of birds in the summer months (Harris et al., 1996). As income breeders, common murres are closely tied to the location of these colonies until their chicks are fledged, and for several weeks after as chicks finish development (Benowitz-Fredericks and Kitaysky, 2005; Hatch, 1983). Species distributions may also vary on fine temporal scales. Common murres distribution patterns are known to shift in response to patchy prey resources – when prey become depleted in one area, birds shift to take advantage of other regions and prey species (Ainley et al., 1996). Thus, the models presented here represent an average seasonal pattern of distribution; divergences from the models predictions may reflect shifting biotic interactions and should be examined from an ecological perspective.

4.3. Limitations

In this study, the only spatial data collected for bird and mammal sightings was transect zone at time of observation, which limited the accuracy of abundance estimates and model training. A standard plot sampling design was used to estimate the abundance of marine bird and mammal species; however, studies show that distance sampling significantly reduces biases in estimated abundance when compared to standard plot sampling by allowing for the calculation of observation bias (Buckland, 2006). This type of sampling would have also provided a clearer result in the case of harbor porpoises, by allowing me to calculate whether the distance at which harbor porpoises could be observed changed between spatial zones. Because the location of individual sightings was not recorded, models had to be trained on values of species density and environmental conditions averaged across each zone (which ranged in size from 0.6 - 2.24 km^{-2}). Thus, the spatial scale of model training was close to but not identical to the scale of model predictions (which occurred across a uniform grid of 1 km^{-2} cells). Distance sampling and/or the collection of more accurate spatial data would have required more extensive observer training which may not have been feasible given the time constraints placed on students in this apprenticeship. Furthermore, the collection of additional data at each bird and mammal sighting may have decreased observers' overall accuracy due to task loading.

The strip transect employed in this study covered a relatively small proportion of my study area, and therefore may not have been totally representative of the species density and environmental conditions in other regions. The results of k-means cluster analysis revealed that our transect line predominantly fell within a single environmental cluster (cluster 3). This in turn suggests that conditions at different points along the transect line are more similar to each other

than to conditions in other regions of my study area. Indeed, the conditions encountered along our transect line were close to the average condition values across my study and did not encompass the full range of values observed across any of my nine environmental variables. This may bias the estimates of abundance for areas in other clusters, particularly in areas with the most extreme values in any given variable. Our transect line does cross the boundaries of two other clusters, clusters 2 and 5 at its northernmost end, and thus, the abundance of predators in these clusters may also be accurately represented in my models. Furthermore, cluster 3, which includes our transect line, was the largest cluster by area (covering 307 km^2) and therefore, my models are likely to be highly accurate across approximately half of my study area at the least. Collection of abundance data from other regions with a wider range of environmental conditions across the SJA will be necessary to fully validate the predictions of my models.

4.4. Conclusions

Species distribution models such as those constructed in this study can not only inform ecological-environmental interactions but can increase the efficacy of conservation efforts by identifying regions of critical importance to marine top predators. Water depth and channel width, the predictive variables most frequently included in my models, highlight the importance of physical habitat structure and suggest that topographic and hydrologic interactions of the SJA create a unique habitat that is highly suitable for marine top predators. My results reflect the dependence of multiple piscivorous predators on populations of forage fish such as Pacific herring and sand lance, and changes in the distribution and abundance of these species could be expected to propagate upwards to higher trophic levels. The highest predicted abundances of marine top predators overlapped in several areas across the SJA, however the majority occurred within 1 km of shore, which suggests that nearshore environments of the SJA are critical habitat to the functioning of the local ecosystem from a top-down perspective. Conservation efforts should therefore be devoted to restoring nearshore habitat and preventing further shoreline degradation in order to preserve suitable habitat for marine predators and their prey. Furthermore, shoreline areas should remain public in order to facilitate public connection to pristine natural spaces and allow equitable access to areas which matter not only to predators, but to people.

Acknowledgements:

For his constant support and mentorship, I would like to extend my most heartfelt gratitude to Dr. Mike Sigler, my primary advisor on this research project. I would also like to thank Dr. Roxanne Carini for her support in connecting with other researchers, processing data, and trouble-shooting challenges throughout the research process. To Drs. Jan Newton and Mathew Baker, I am deeply indebted not only for their outstanding mentorship but for their efforts in developing and maintaining this research apprenticeship as an outstanding educational opportunity for young scientists. Thank you to Nicole Frederick for your advice and encouragement throughout the data analysis and writing process and for always challenging me to do better. Thank you to Erica Diane Merto, Jazzy Shepard, Jerry Liu, Dylan Greenwald, Donovan Hesselroth, and Connor Trentman for volunteering your assistance observing and recording the abundance of marine bird and mammal species on our annual transect, your assistance made the collection of our data possible. To my friends, Andrew Fletcher, Henry Siahaan, Madeline Kopf-Patterson, and Kennadie Selden, thank you for the many smiles you

brought to my face these past 10 weeks and for inspiring me with your outstanding research. Thank you to Jakob Beuche and Kristy Kull for their outstanding work operating the R/V Kittiwake and for conducting us safely along our surveys each week, and to all of the faculty and staff at Friday Harbor Labs who make it possible to conduct research in this, one of the most unique coastal ecosystems in the world. Lastly, thank you to all the PEF apprentice's past and future for your role carrying the torch of scientific discovery – you are the searchlight in the unknown. I would like to acknowledge the support of the Mary Gates Endowment Scholarship in this research.

References:

Ainley, D.G., Spear, L.B., Allen, S.G., Ribic, C.A., 1996. Temporal and Spatial Patterns in the Diet of the Common Murre in California Waters. The Condor 98, 691–705. https://doi.org/10.2307/1369852

Alava, J.J., 2019. Legacy and Emerging Pollutants in Marine Mammals' Habitat from British Columbia, Canada: Management perspectives for sensitive marine ecosystems. pp. 87–114. https://doi.org/10.1201/9780429025303

Ashe, E., 2020. Dolphins and herring of the Salish Sea: understanding responses of a top predator to fluctuating prey and human disturbance. Salish Sea Ecosyst. Conf.

Baker, M.R., Williams, K., Greene, H.G., Greufe, C., Lopes, H., Aschoff, J., Towler, R., 2021. Use of manned submersible and autonomous stereo-camera array to assess forage fish and associated subtidal habitat. Fish. Res. 243, 106067. https://doi.org/10.1016/j.fishres.2021.106067

Benowitz-Fredericks, Z.M., Kitaysky, A.S., 2005. Benefits and costs of rapid growth in common murre chicks Uria aalge. J. Avian Biol. 36, 287–294. https://doi.org/10.1111/j.0908-8857.2005.03357.x

Bertram, D., 2020. A baseline of seasonal changes in the at sea distribution and abundance of marine birds near shipping lanes around southern Vancouver Island. Salish Sea Ecosyst. Conf.

Block, B.A., Jonsen, I.D., Jorgensen, S.J., Winship, A.J., Shaffer, S.A., Bograd, S.J., Hazen, E.L., Foley, D.G., Breed, G.A., Harrison, A.-L., Ganong, J.E., Swithenbank, A., Castleton, M., Dewar, H., Mate, B.R., Shillinger, G.L., Schaefer, K.M., Benson, S.R., Weise, M.J., Henry, R.W., Costa, D.P., 2011. Tracking apex marine predator movements in a dynamic ocean. Nature 475, 86–90. https://doi.org/10.1038/nature10082

Boldt, J.L., Canada, Department of Fisheries and Oceans, 2019. State of the Physical, biological and selected fishery resources of Pacific Canadian marine ecosystems in 2018.

Buckland, S.T., 2006. Point-Transect Surveys for Songbirds: Robust Methodologies. The Auk 123, 345–357. https://doi.org/10.1093/auk/123.2.345

Elliser, C.R., Hall, A., 2021. Return of the Salish Sea Harbor Porpoise, Phocoena phocoena: Knowledge Gaps, Current Research, and What We Need to Do to Protect Their Future. Front. Mar. Sci. 8, 534. https://doi.org/10.3389/fmars.2021.618177

Elliser, C.R., Hessing, S., MacIver, K.H., Webber, M.A., Keener, W., 2020. Harbor Porpoises (Phocoena phocoena vomerina) Catching and Handling Large Fish on the U.S. West Coast. Aquat. Mamm. 46, 191–199. https://doi.org/10.1578/AM.46.2.2020.191

Feddern, M.L., Holtgrieve, G.W., Ward, E.J., 2021. Stable isotope signatures in historic harbor seal bone link food web-assimilated carbon and nitrogen resources to a century of

environmental change. Glob. Change Biol. 27, 2328–2342. https://doi.org/10.1111/gcb.15551
Feely, R.A., Klinger, T., 1956-, Newton, J.A. (Jan A.), Chadsey, Meg., 2012. Scientific summary of ocean acidification in Washington State marine waters. NOAA OAR special report.
Feng, C., Liang, W., 2020. Behavioral responses of black-headed gulls (Chroicocephalus ridibundus) to artificial provisioning in China. Glob. Ecol. Conserv. 21, e00873. https://doi.org/10.1016/j.gecco.2019.e00873
Ferrier, S., 2002. Mapping Spatial Pattern in Biodiversity for Regional Conservation Planning: Where to from Here? Syst. Biol. 51, 331–363. https://doi.org/10.1080/10635150252899806
Fletcher, A., 2021. Dietary and Spatial Analysis of Salmon in the San Juan Archipelago and the Salish Sea. Pelagic Ecosyst. Funct. Res. Apprenticesh.
Frederick, N., 2021. Impacts of tidal current and fish density on spatial distribution of harbor seal (Phoca vitulina) and harbor porpoise (Phocoena phocoena) in San Juan Channel. Pelagic Ecosyst. Funct. Res. Apprenticesh.
Gause, G.F., 1971. The Struggle for Existence 129.
Gause, G.F., 1934. Experimental Analysis of Vito Volterra's Mathematical Theory of the Struggle for Existence. Sci. New Ser. 79, 16–17.
Gaydos, J.K., Pearson, S.F., 2011. Birds and Mammals that Depend on the Salish Sea: A Compilation. Northwest. Nat. 92, 79–94. https://doi.org/10.1898/10-04.1
Gilles, A., Viquerat, S., Becker, E.A., Forney, K.A., Geelhoed, S.C.V., Haelters, J., Nabe-Nielsen, J., Scheidat, M., Siebert, U., Sveegaard, S., van Beest, F.M., van Bemmelen, R., Aarts, G., 2016. Seasonal habitat-based density models for a marine top predator, the harbor porpoise, in a dynamic environment. Ecosphere 7, e01367. https://doi.org/10.1002/ecs2.1367
Gobler, C.J., Doherty, O.M., Hattenrath-Lehmann, T.K., Griffith, A.W., Kang, Y., Litaker, R.W., 2017. Ocean warming since 1982 has expanded the niche of toxic algal blooms in the North Atlantic and North Pacific oceans. Proc. Natl. Acad. Sci. 114, 4975–4980. https://doi.org/10.1073/pnas.1619575114
Greene, H.G., Baker, M., Aschoff, J., 2020. Chapter 14 - A dynamic bedforms habitat for the forage fish Pacific sand lance, San Juan Islands, WA, United States, in: Harris, P.T., Baker, E. (Eds.), Seafloor Geomorphology as Benthic Habitat (Second Edition). Elsevier, pp. 267–279. https://doi.org/10.1016/B978-0-12-814960-7.00014-2
Guisan, A., Edwards, T.C., Hastie, T., 2002. Generalized linear and generalized additive models in studies of species distributions: setting the scene. Ecol. Model. 157, 89–100. https://doi.org/10.1016/S0304-3800(02)00204-1
Guisan, A., Thuiller, W., 2005. Predicting species distribution: offering more than simple habitat models. Ecol. Lett. 8, 993–1009. https://doi.org/10.1111/j.1461-0248.2005.00792.x
Gulka, J., Ronconi, R.A., Davoren, G.K., 2019. Spatial segregation contrasting dietary overlap: niche partitioning of two sympatric alcids during shifting resource availability. Mar. Biol. 166, 115. https://doi.org/10.1007/s00227-019-3553-x
Harris, M.P., Wanless, S., Barton, T.R., 1996. Site use and fidelity in the Common Guillemot Uria aalge. Ibis 138, 399–404. https://doi.org/10.1111/j.1474-919X.1996.tb08057.x
Harvey, C.J., Williams, G.D., Levin, P.S., 2012. Food Web Structure and Trophic Control in Central Puget Sound. Estuaries Coasts 35, 821–838. https://doi.org/10.1007/s12237-012-9483-1

Hastie, T.J., Tibshirani, R.J., 1990. Generalized Additive Models. Routledge, Boca Raton. https://doi.org/10.1201/9780203753781
Hatch, S., 1983. THE FLEDGING OF COMMON AND THICK-BILLED MURRES ON MIDDLETON ISLAND, ALASKA. J. Field Ornithol. 54, 266–274.
Hazen, E.L., Abrahms, B., Brodie, S., Carroll, G., Jacox, M.G., Savoca, M.S., Scales, K.L., Sydeman, W.J., Bograd, S.J., 2019. Marine top predators as climate and ecosystem sentinels. Front. Ecol. Environ. 17, 565–574. https://doi.org/10.1002/fee.2125
Hazen, E.L., Scales, K.L., Maxwell, S.M., Briscoe, D.K., Welch, H., Bograd, S.J., Bailey, H., Benson, S.R., Eguchi, T., Dewar, H., Kohin, S., Costa, D.P., Crowder, L.B., Lewison, R.L., 2018. A dynamic ocean management tool to reduce bycatch and support sustainable fisheries. Sci. Adv. 4, eaar3001. https://doi.org/10.1126/sciadv.aar3001
Hosmer, D.W., Lemeshow, S., Sturdivant, R.X., 1989. Applied Logistic Regression. John Wiley & Sons.
Huyer, A., 1983. Coastal upwelling in the California current system. Prog. Oceanogr. 12, 259–284. https://doi.org/10.1016/0079-6611(83)90010-1
Irons, D.B., 1998. Foraging Area Fidelity of Individual Seabirds in Relation to Tidal Cycles and Flock Feeding. Ecology 79, 647–655. https://doi.org/10.1890/0012-9658(1998)079[0647:FAFOIS]2.0.CO;2
Johnston, D., Westgate, A., Read, A., 2005. Effects of fine-scale oceanographic features on the distribution and movements of harbour porpoises Phocoena phocoena in the Bay of Fundy. Mar. Ecol. Prog. Ser. 295, 279–293. https://doi.org/10.3354/meps295279
Kassambara, A., Mundt, F., 2020. factoextra: Extract and Visualize the Results of Multivariate Data Analyses.
Lance, M.M., Thompson, C.W., 2005. Overlap in Diets and Foraging of Common Murres (Uria Aalge) and Rhinoceros Auklets (Cerorhinca Monocerata) After the Breeding Season. The Auk 122, 887–901. https://doi.org/10.1093/auk/122.3.887
Leathwick, J., Austin, M., 2001. Competitive Interactions between Tree Species in New Zealand's Old-Growth Indigenous Forests. Ecology 82, 2560–2573. https://doi.org/10.2307/2679936
Marubini, F., Gimona, A., Evans, P., Wright, P., Pierce, G., 2009. Habitat preferences and interannual variability in occurrence of the harbour porpoise Phocoena phocoena off northwest Scotland. Mar. Ecol. Prog. Ser. 381, 297–310. https://doi.org/10.3354/meps07893
Mofjeld, H.O., Larsen, L.H., 1984. Tides and tidal currents of the inland waters of western Washington.
Nichol, L.M., Hall, A.M., Ellis, G.M., Stredulinsky, E., Boogaards, M., Ford, J.K.B., 2013. Dietary overlap and niche partitioning of sympatric harbour porpoises and Dall's porpoises in the Salish Sea. Prog. Oceanogr., Strait of Georgia Ecosystem Research Initiative (ERI) 115, 202–210. https://doi.org/10.1016/j.pocean.2013.05.016
Olson, J.K., Lambourn, D.M., Huggins, J.L., Raverty, S., Scott, A.A., Gaydos, J.K., 2021. Trends in Propeller Strike-Induced Mortality in Harbor Seals (Phoca vitulina) of the Salish Sea. J. Wildl. Dis. 57, 689–693. https://doi.org/10.7589/JWD-D-20-00221
Pearce, J., Ferrier, S., 2000. An evaluation of alternative algorithms for fitting species distribution models using logistic regression. Ecol. Model. 128, 127–147. https://doi.org/10.1016/S0304-3800(99)00227-6

Piatt, J.F., Nettleship, D.N., 1985. Diving Depths of Four Alcids. The Auk 102, 293–297. https://doi.org/10.2307/4086771
QGIS Development Team, 2021. QGIS Geographic Information System. QGIS Association.
R Core Team, 2019. R: A Language and Environment for Statistical Computing. R Foundation for Statistical Computing, Vienna, Austria.
Rice, C.A., 2006. Effects of shoreline modification on a Northern Puget Sound beach: Microclimate and embryo mortality in surf smelt (Hypomesus pretiosus). Estuaries Coasts 29, 63. https://doi.org/10.1007/BF02784699
Riedman, M., 1990. The Pinnipeds: Seals, Sea Lions, and Walruses. University of California Press.
Schulien, J.A., Adams, J., Felis, J.J., 2020. Pacific Continental Shelf Environmental Assessment (PaCSEA): Characterization of Seasonal Water Masses within the Northern California Current System Using Airborne Remote Sensing off Northern California, Oregon, and Washington, 2011-2012 35.
Scott, B.E., Sharples, J., Ross, O.N., Wang, J., Pierce, G.J., Camphuysen, C.J., 2010. Sub-surface hotspots in shallow seas: fine-scale limited locations of top predator foraging habitat indicated by tidal mixing and sub-surface chlorophyll. Mar. Ecol. Prog. Ser. 408, 207–226. https://doi.org/10.3354/meps08552
Selden, K., 2021. Spatial Comparison of Microplastics in Benthic and Pelagic Fish: A San Juan Archipelago Study. Pelagic Ecosyst. Funct. Res. Apprenticesh.
Shaffer, S.A., Tremblay, Y., Weimerskirch, H., Scott, D., Thompson, D.R., Sagar, P.M., Moller, H., Taylor, G.A., Foley, D.G., Block, B.A., Costa, D.P., 2006. Migratory shearwaters integrate oceanic resources across the Pacific Ocean in an endless summer. Proc. Natl. Acad. Sci. 103, 12799–12802. https://doi.org/10.1073/pnas.0603715103
Spyrakos, E., Santos-Diniz, T.C., Martinez-Iglesias, G., Torres-Palenzuela, J.M., Pierce, G.J., 2011. Spatiotemporal patterns of marine mammal distribution in coastal waters of Galicia, NW Spain. Hydrobiologia 670, 87. https://doi.org/10.1007/s10750-011-0722-4
Stasko, A.B., Horrall, R.M., Hasler, A. d., 1976. Coastal Movements of Adult Fraser River Sockeye Salmon (Oncorhynchus nerka) Observed by Ultrasonic Tracking. Trans. Am. Fish. Soc. 105, 64–71. https://doi.org/10.1577/1548-8659(1976)105<64:CMOAFR>2.0.CO;2
Teilmann, J., Galatius, A., 2018. Harbor Seal: Phoca vitulina, in: Würsig, B., Thewissen, J.G.M., Kovacs, K.M. (Eds.), Encyclopedia of Marine Mammals (Third Edition). Academic Press, pp. 451–455. https://doi.org/10.1016/B978-0-12-804327-1.00145-X
Tynan, C.T., Ainley, D.G., Barth, J.A., Cowles, T.J., Pierce, S.D., Spear, L.B., 2005. Cetacean distributions relative to ocean processes in the northern California Current System. Deep Sea Res. Part II Top. Stud. Oceanogr., U.S. GLOBEC Biological and Physical Studies of Plankton, Fish and Higher Trophic Level Production, Distribution, and Variability in the Northeast Pacific 52, 145–167. https://doi.org/10.1016/j.dsr2.2004.09.024
Wagenmakers, E.-J., Farrell, S., 2004. AIC model selection using Akaike weights. Psychon. Bull. Rev. 11, 192–196. https://doi.org/10.3758/BF03206482
Wood, S.N., 2003. Thin plate regression splines. J. R. Stat. Soc. Ser. B Stat. Methodol. 65, 95–114. https://doi.org/10.1111/1467-9868.00374
Zamon, J., 2003. Mixed species aggregations feeding upon herring and sandlance schools in a nearshore archipelago depend on flooding tidal currents. Mar. Ecol. Prog. Ser. 261, 243–255. https://doi.org/10.3354/meps261243

Zamon, J.E., 2002. Tidal changes in copepod abundance and maintenance of a summer Coscinodiscus bloom in the southern San Juan Channel, San Juan Islands, USA. Mar. Ecol. Prog. Ser. 226, 193–210. https://doi.org/10.3354/meps226193

Zamon, J.E., 2001. Seal predation on salmon and forage fish schools as a function of tidal currents in the San Juan Islands, Washington, USA: Seal predation on salmon and forage fish. Fish. Oceanogr. 10, 353–366. https://doi.org/10.1046/j.1365-2419.2001.00180.x

Tables and Figures:

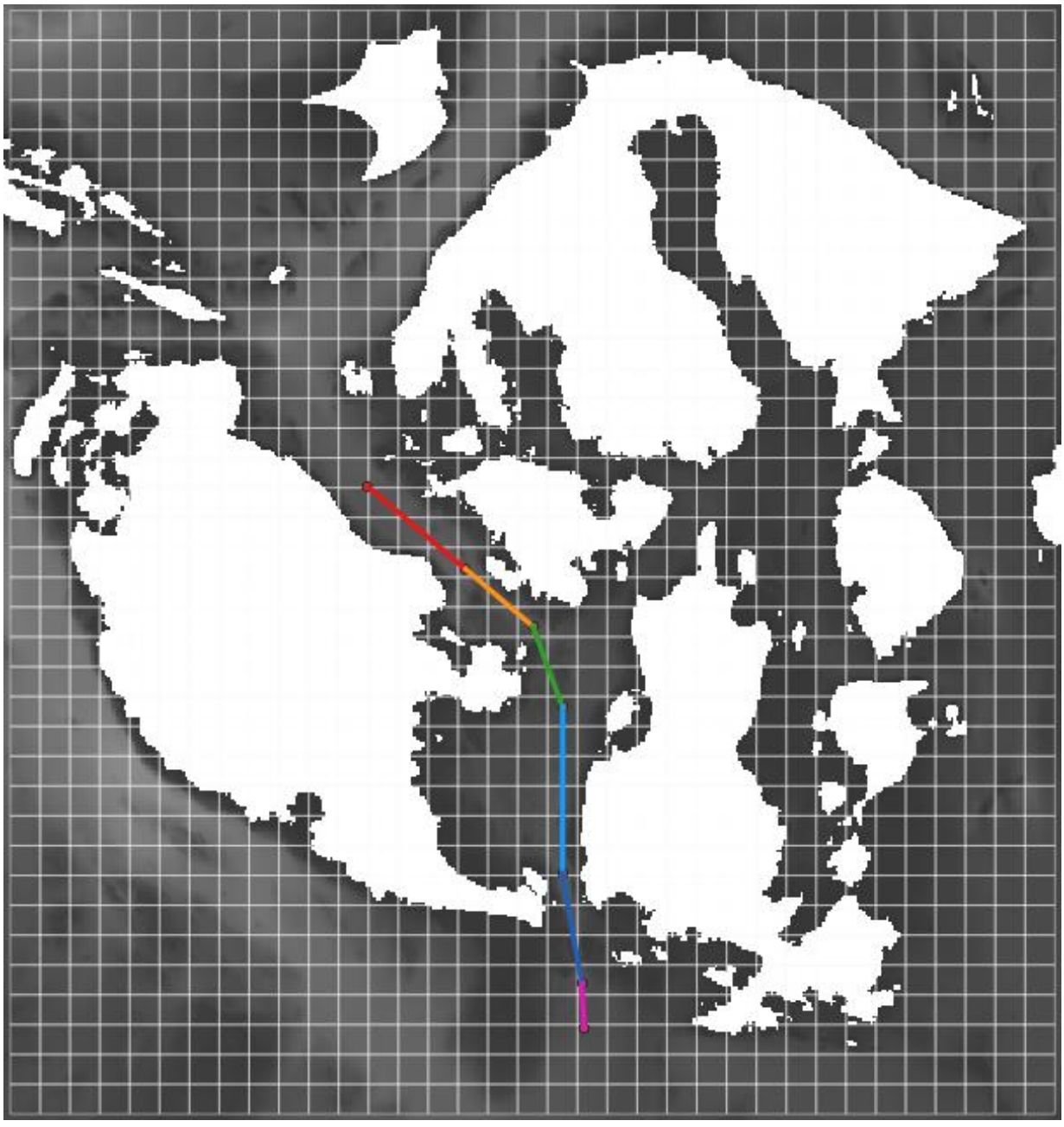

Figure 1: Map of study area with grid cells and transect lines marked. The transect line is divided into zones with zone 1 (red), zone 2 (gold), zone 3 (green), zone 4 (teal), zone 5, (navy), and zone 6 (pink).

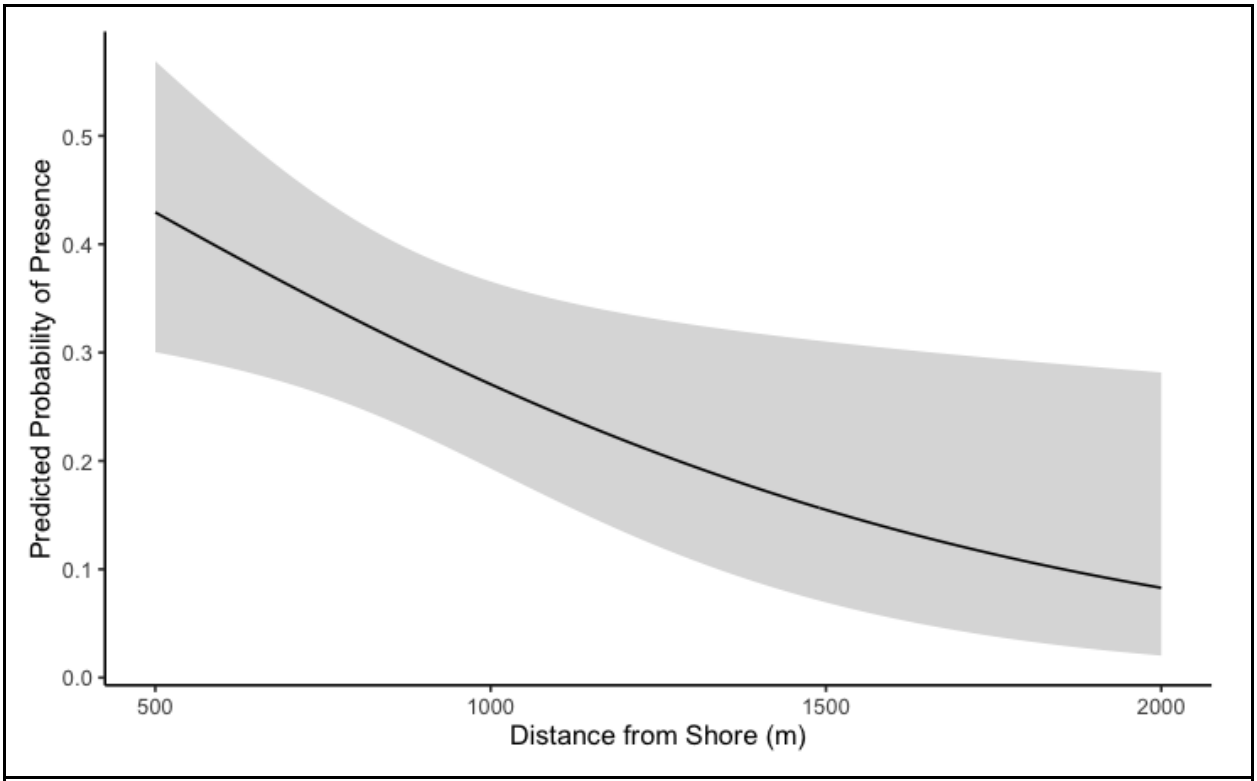

Figure 2: Logistic regression results of the best predictive model for harbor porpoises, displaying the modeled change in probability of habitat occupancy by porpoises (y-axis) relative to the only significant explanatory variable for this species, distance from shore (x-axis).

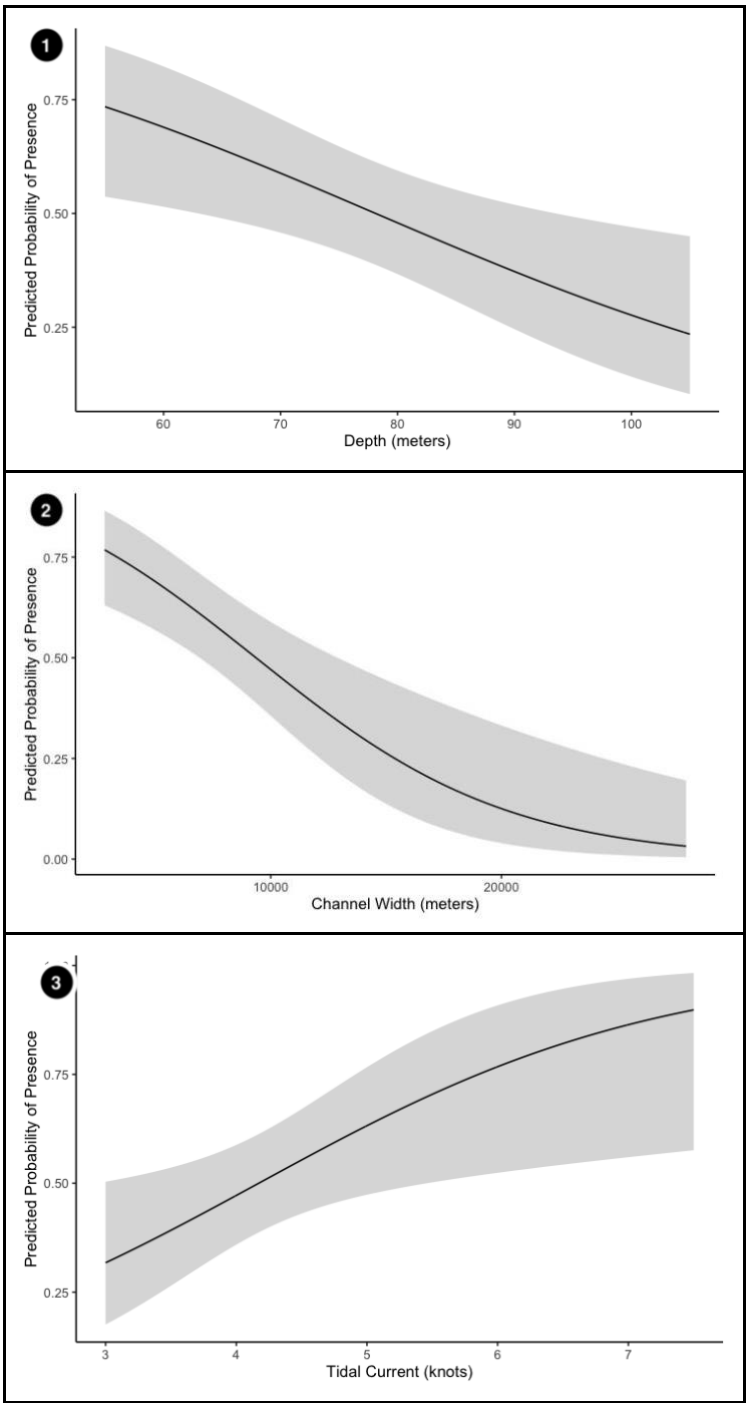

Figure 3: Logistic regression results of the best predictive model for harbor seals, displaying the modeled change in probability of habitat occupancy by seals (y-axis) relative to significant environmental predictors depth (1), channel width (2), and tidal current amplitude (3)(x-axis).

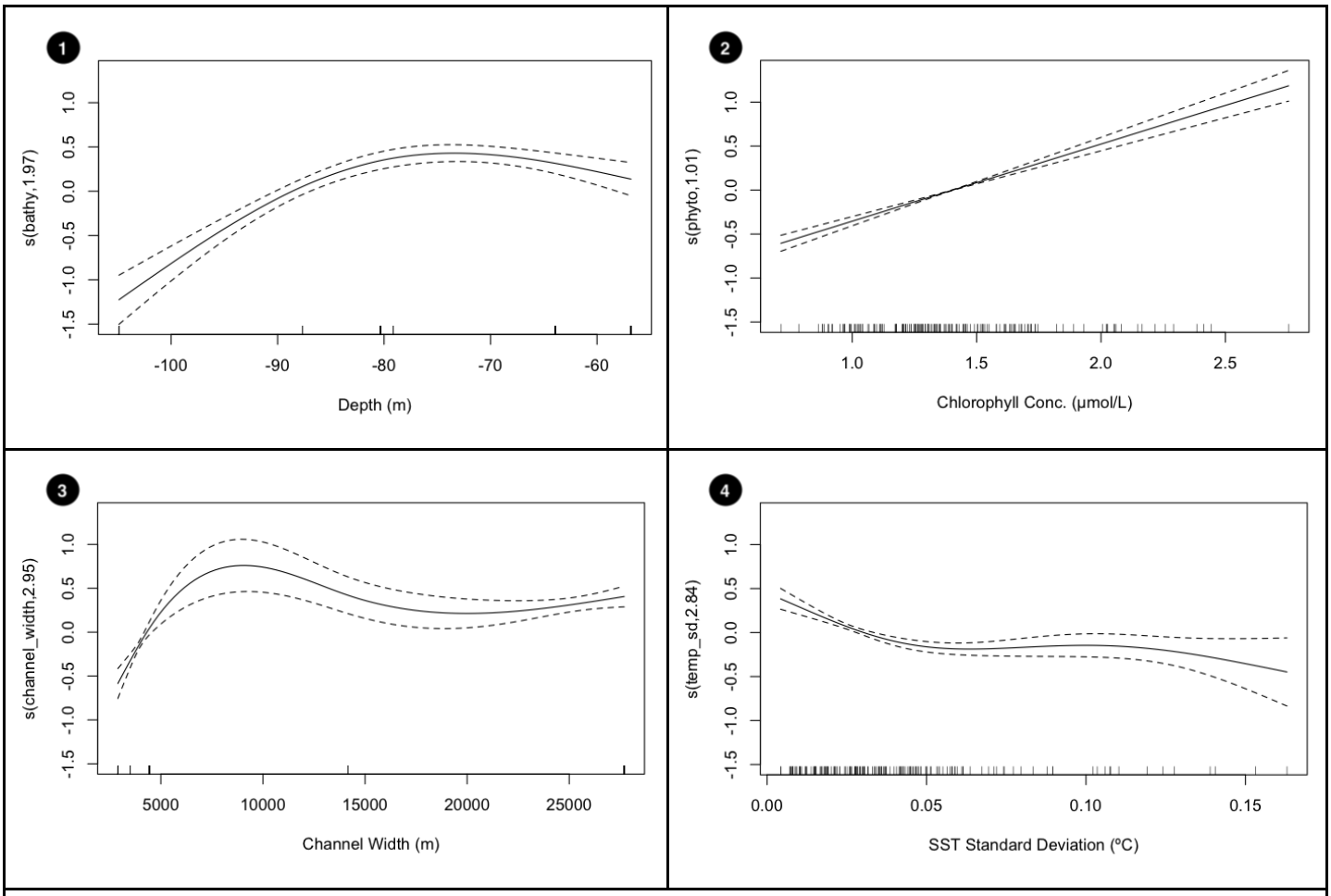

Figure 4: GAM results of the best predictive model for common murres, displaying the modeled change in murre density(y-axis) relative to significant environmental predictors depth (1), chlorophyll concentration (2), channel width (3), and SST standard deviation (4). Dotted lines represent 2 SE interval around the mean prediction. Vertical marks along the x-axis represent the distribution of values included in model training.

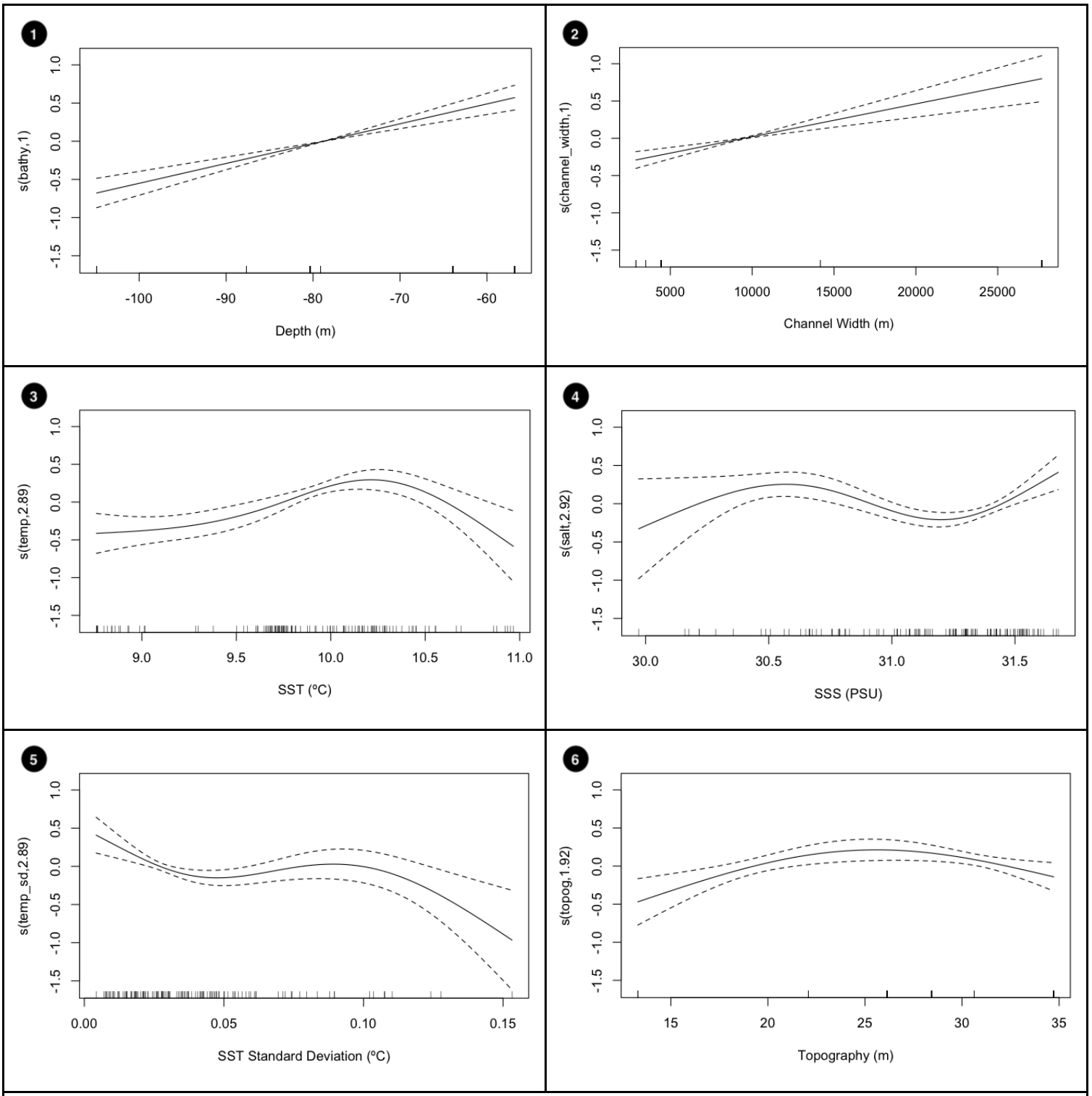

Figure 5: GAM results of the best predictive model for glaucous winged gulls, displaying the modeled change in gull density(y-axis) relative to significant environmental predictors depth (1), channel width (2), temperature (3), salinity (4), SST standard deviation (5), and topography (6). Dotted lines represent 2 SE interval around the mean prediction. Vertical marks along the x-axis represent the distribution of values included in model training.

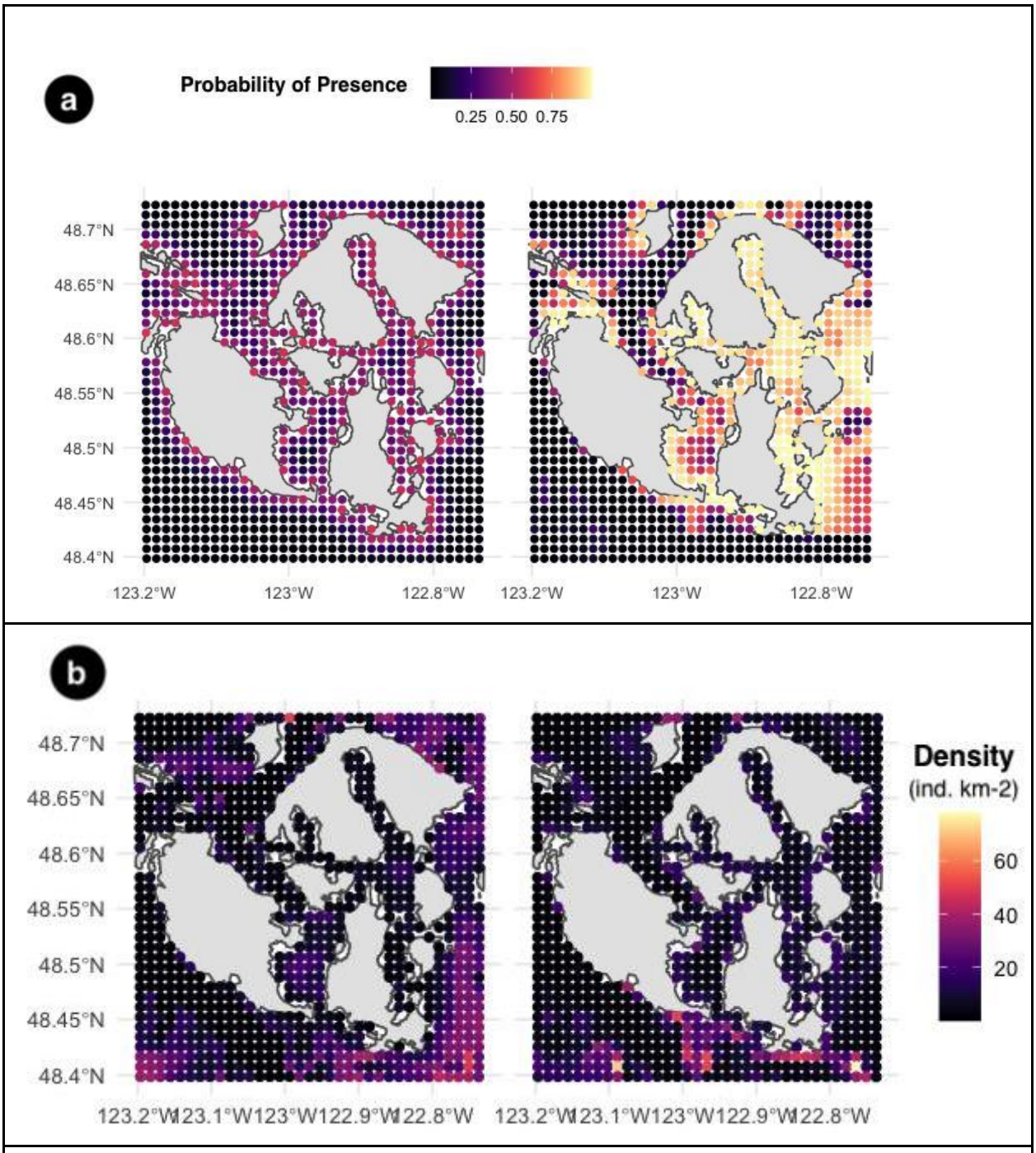

Figure 6: Predicted habitat maps for marine top predators in the San Juan Archipelago. a. Predicted probabilities of habitat occupancy based on logistic regression models of marine mammal distribution (L: harbor porpoise, R: harbor seals). b. Predicted species densities for seabirds based on generalized additive models (L: common murre, R: glaucous-winged gull).

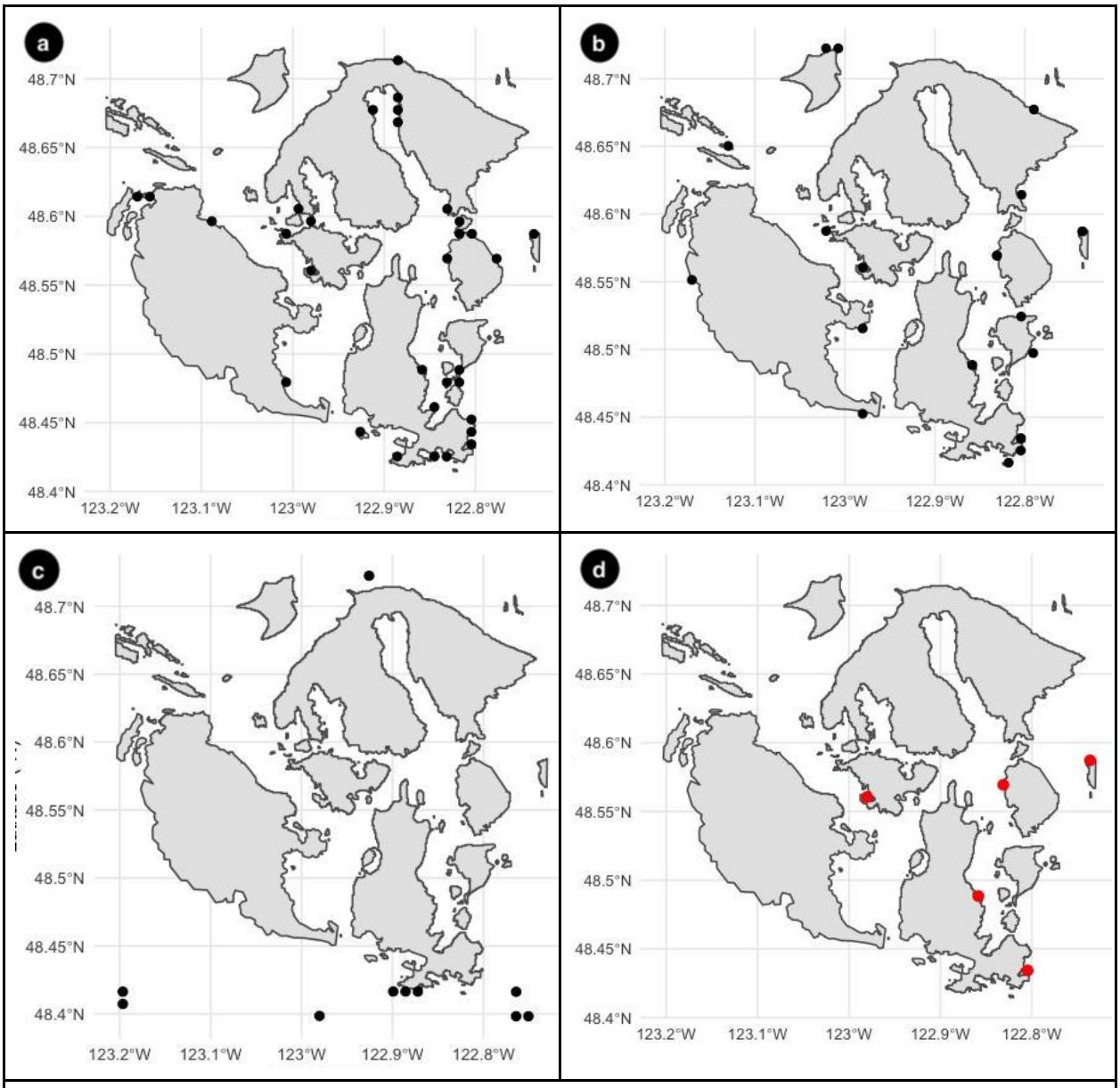

Figure 7: Locations of core habitat overlap as identified by the 90th percentile of predicted abundance for each predator species. a. Overlap between marine mammal species occurs near shallow bays, sounds, and current hotspots. b. Overlap between marine mammals and seabirds occurs near beaches, banks and bays with highly varied conditions. c. Overlap between seabird species occurs in broad channels and straits. d. Core habitat overlap between three predator species indicate regions of the highest importance for marine mammals in my study area.

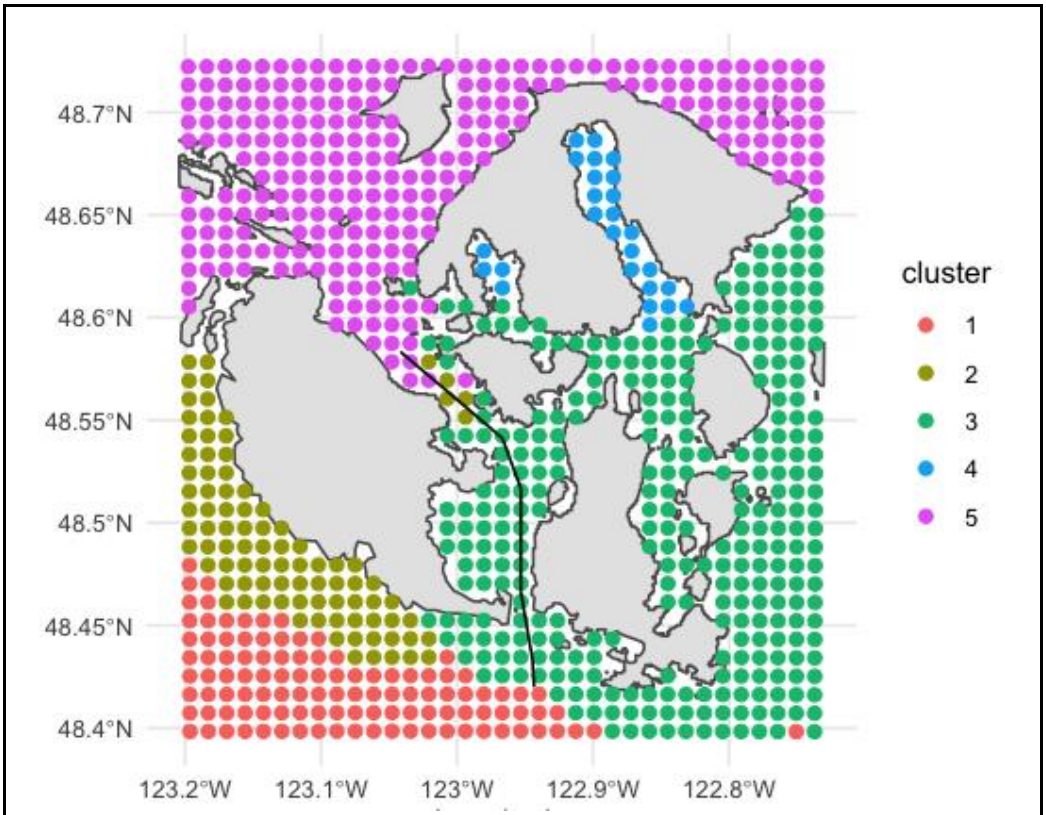

Figure 8: Spatial distribution of environmental clusters identified using k-means clustering. Marine bird and mammal transect line, depicted in black, occurs predominantly in cluster 3 but passes into clusters 2 and 5 at its northern end.

Table 1: Spatial metadata for zones of the Pelagic Ecosystem Function marine bird and mammal transect line including spatial bounds and lengths. The coordinates for the north and south oceanographic stations are highlighted in grey.

Zone (n)	**Start Lat. (ºN)**	**Start Lon. (ºW)**	**End Lat. (ºN)**	**End Lon. (ºW)**	**Length (km)**
1	48.583	123.048	48.550	122.999	5
2	48.550	122.999	48.533	122.966	3
3	48.533	122.966	48.516	122.958	2
4	48.516	122.958	48.466	122.950	6
5	48.466	122.950	48.433	122.953	4
6	48.433	122.953	48.422	122.950	1

Table 2: List of environmental variables considered in our habitat model and their data sources. Spatial and temporal resolution of the innate data source before processing are given for each variable.

	Code	Variable	Data Source	Spatial Resolution	Temporal Resolution
Static Variables	BA	bathymetry	U.S. Coastal Relief Model	90 meters	-
	TO	Bathymetry standard Deviation	U.S. Coastal Relief Model	90 meters	-
	DS	Distance from shore	Calculated	$1km^2$	-
	CS	Channel width	Calculated	$1km^2$	-
	TC	Tidal current amplitude	NOAA Tide Stations	Point (40x)	24-hours
Dynamic Variables	SSS	Salinity	LiveOcean	$< 1km^2$	24-hour
	SST	Sea surface temperature	LiveOcean	$< 1km^2$	24-hour
	T-SD	Sea surface temperature standard deviation	LiveOcean	$< 1km^2$	24-hour
	CHL	Chlorophyll-a irradiance	LiveOcean	$< 1km^2$	24-hour

Table 3: Pearson linear correlation coefficients (r) between explanatory environmental variables [a], n = 221,392 grid cells across October to November from 2017-2021.

	BA	TO	DS	CW	TC	CHL	SST	T-SD
TO	-0.20							
DS	-0.20	-0.26						
CW	-0.16	-0.12	**0.66**					
TC	0.18	-0.07	0.07	0.09				
CHL	0.18	-0.12	-0.12	-0.08	-0.01			
SST	0.01	*-0.01*	-0.06	-0.07	-0.06	**0.73**		
T-SD	-0.07	0.08	-0.05	-0.05	-0.06	0.25	0.39	
SSS	0.04	-0.04	0.12	0.14	0.14	**-0.52**	-0.39	-0.27

[a] **Bolded** values represent correlations of moderate to high strength ($|r| \geq 0.5$). *Italicized* value represents the singular r value which was not statistically significant ($\alpha > 0.05$). BA, bathymetry; TO, topography, DS distance to shore; CW, channel width; TC tidal current amplitude; CHL, chlorophyll concentration; SST, sea-surface temperature; T-SD, standard deviation of sea surface temperature; SSS, sea surface salinity.

Table 4: Summary statistics for survey effort, predator abundance, and environmental conditions between years. Data are number of transects conducted, cumulative area surveyed, proportion of transect zones in which marine mammals were observed, mean value and range for all other variables.

Year	Transects (n)	Cumulative area surveyed (km^{-2})	Proportion mammal presence	Seabird density (indiv. km^{-2})	SST (ºC)	T-SD (ºC)	CHL (µmol/L)	SSS (PSU)
2017	12	103.2	0.31	9 (0 – 38)	9.7 (8.7 – 11)	0.03 (0.00 – 0.14)	1.5 (0.78 – 2.8)	31 (29 – 31)
2018	12	103.2	0.36	10 (0 – 38)	10 (9.6 – 10)	0.05 (0.01 – 0.10)	1.4 (0.86 – 2.1)	31 (30 – 31)
2019	10	86	0.55	10 (1 – 38)	9.8 (9.2 – 11)	0.03 (0.00 – 0.15)	1.3 (0.99 – 1.7)	31 (30 – 31)
2020	14	120.4	0.44	9 (0 – 38)	9.9 (8.8 – 11)	0.04 (0.01 – 0.16)	1.4 (0.96 – 2.0)	30 (28 – 31)
2021	8	68.8	0.31	12 (0 – 27)	9.7 (9.4 – 10)	0.03 (0.00 – 0.10)	1.2 (0.71 – 1.7)	31 (30 – 31)

Table 5: Results of the logistic regression predicting marine mammal presence and generalized additive models predicting seabird density with the highest fit *edf* is estimated degrees of freedom.

	Estimate	SE	p
Harbor Porpoise			
DS	-0.0014	0.0006	0.0223
Harbor Seal			
BA	0.0439	0.0163	0.0072
CW	-0.0001	4.94×10^{-5}	0.0002
TC	0.6535	0.2768	0.0182

	edf	$\chi 2$	p
Glaucous-winged gull			
s(BA)	1.000	49.72	< 0.0001
s(CW)	1.000	27.05	< 0.0001
s(SST)	2.891	29.56	< 0.0001
s(SSS)	2.921	21.70	< 0.0001
s(T-SD)	2.895	15.70	0.001
s(TO)	1.916	10.67	0.005
Common Murre			
s(BA)	1.973	82.92	< 0.0001
s(CHL)	1.009	189.25	< 0.0001
s(CW)	2.951	117.45	< 0.0001
s(T-SD)	2.838	48.06	< 0.0001

Table 6: Summary of mean values for environmental conditions within each spatial cluster

Cluster (n)	**BA (m)**	**TO (m)**	**DS (km)**	**CW (km)**	**TC (kn)**	**CHL (µmol/L)**	**SST (ºC)**	**T-SD (ºC)**	**SSS (PSU)**
1	91.5	11.8	6.24	33.4	3.95	1.21	9.54	0.028	31.2
2	179	30.3	1.90	16.3	3.85	1.14	9.54	0.035	31.2
3	48.4	11.6	1.33	11.4	4.53	1.42	9.65	0.026	31.0
4	21.2	7.24	0.467	2.31	3.51	2.26	9.90	0.028	31.1
5	96.2	20.7	1.30	9.69	2.98	1.31	9.86	0.046	30.4